

# Content based COVID-19 image retrieval system using local histogram equalization and deep convolutional neural network

Rani Shetty<sup>1</sup>, Vandana S. Bhat<sup>2</sup>, Jagadeesh Pujari<sup>3</sup>, Rashmi Shetty<sup>4</sup>

<sup>1</sup>Department of Computer Science and Engineering, SDM College of Engineering and Technology, Dharwad, Visveswaraya Technical University, Karnataka, India

<sup>2</sup>Department of Artificial Intelligence and Machine Learning, SDM College of Engineering and Technology, Dharwad, Visveswaraya Technical University, Karnataka, India

<sup>3</sup>Department of Information Science and Engineering, SDM College of Engineering and Technology, Dharwad, Visveswaraya Technical University, Karnataka, India

<sup>4</sup>Department of Pathology, Kasturba Medical College Manipal, Karnataka, India

## Article Info

### Article history:

Received Nov 4, 2023

Revised Mar 19, 2024

Accepted Apr 2, 2024

### Keywords:

Content based medical image retrieval

Convolutional neural network

Feature extraction

Image retrieval

Similarity measure

## ABSTRACT

Doctors play a critical role in interpreting medical images as part of their core responsibilities. They need to find comparable examples that can assist in making informed decisions, especially when encountering ambiguous visuals. Traditionally, Systems such as content-based medical image retrieval (CBMIR) have been used for this. The proposed method employs a novel technique, local histogram equalization (LHE) for preprocessing, transfer learning-based convolutional neural network to extract the representative features with Manhattan and Euclidean distance metrics to assess how similar the query image and database image are to one another. This model is trained on a standard dataset namely Chest X-Ray images. Top-k, Precision and Recall measure is employed to assess system performance. From the results, the suggested enhanced convolutional neural network (CNN) model demonstrates significantly superior performance in the top 10 retrieval rates of 97.13% for coronavirus disease 2019 (COVID-19), 96.84% for normal, 82.63% for pneumonia-bacterial, and 81.72% for pneumonia-viral and precision@recall10 of 93.14% for COVID-19, 91.88% for normal, 77.84% for pneumonia-bacterial and 74.71% for pneumonia-viral.

*This is an open access article under the [CC BY-SA](https://creativecommons.org/licenses/by-sa/4.0/) license.*



## Corresponding Author:

Rani Shetty

Department of Computer Science and Engineering, SDM College of Engineering and Technology, Dharwad, Visveswaraya Technical University

Dharwad 580002, Karnataka, India

Email: ranishetty1990@sdmcet.ac.in

## 1. INTRODUCTION

Clinical medicine depends heavily on imaging for tasks including diagnosis, care, planning, and monitoring patient response [1]. Image similarity holds significant importance in medical practice as diagnostic [2], [3] decision-making traditionally relies on patient information, including both images and non-image data. Recently, digital images have gained popularity across numerous disciplines, including education, science, and medicine [4]. Hospitals and medical facilities generate a substantial volume of digital images as part of their daily operations, including X-rays, mammograms, and magnetic resonance imaging (MRI) [5]. Numerous researchers have opted to employ content-based image retrieval systems as their primary method for locating images with similar content [6], [7]. content based medical image retrieval (CBMIR) is particularly effective for medical images since it relies on visual characteristics to measure

similarity, unlike text-based image retrieval approaches [8] that necessitate annotated medical images. In the context of chest X-rays [9], [10], an individual image may encompass various diseases, making it impractical to report each one in every instance. Various existing methods use handcrafted techniques for image retrieval tasks [11], [12].

Machine learning research [13] has advanced significantly, especially since the deep learning framework was introduced. A wide variety of advanced machine learning methods known as “deep learning” enable the modeling of sophisticated abstractions in data [14]. This is achieved using deep architectures consisting of multiple nonlinear transformations. Deep learning emulates the intricate structure of the human brain [15], where information is processed through numerous layers of transformation. Consequently, deep learning methods offer a direct means of automatically learning features [16] at several levels of abstraction by exploring deep architectures. These techniques enable the system to acquire sophisticated features from raw images without relying on manually crafted features. Recent investigations have proven the successful application of deep learning techniques across various domains, including image and video classification [17], [18], visual tracking [19], speech recognition [20], and natural language processing [21]. Recently, researchers have explored the practice of techniques like deep learning in CBMIR tasks, as evidenced by several studies [22]. The study employs a global categorization approach, where images of various body parts are grouped into distinct classes [23], [24] each labeled corresponding to the body component.

The content-based coronavirus disease 2019 (COVID-19) image retrieval system is an important pandemic tool with numerous benefits. It assists clinicians by acting as a visual aid in diagnoses and facilitates decision-making [25], [26] by comparing patient images to a database of confirmed cases. Here, we concentrate on the issue of medical image retrieval. COVID-19 can induce gradual respiratory failure in individuals, leading to hospitalization and possible death. This study’s major goal is to characterize the COVID-19 feature discovered in chest X-ray images using a mix of local histogram equalization (LHE) and an efficient deep learning model that can beat existing manual approaches. The study presents three significant contributions: i) the utilization of transfer learning on various convolutional neural networks and image augmentation enhances robustness and generalization in medical imaging, ii) a novel deep convolutional neural network (CNN) model with optimized preprocessing techniques for efficient feature extraction using a collection of medical images, and iii) leveraging the acquired features to build an extremely effective retrieval approach for medical images using graphics processing units (GPUs) capable of handling vast datasets.

To facilitate comprehension, this paper is arranged as follows: section 2 describes the proposed method. Section 3 details the suggested experimental setting, including results and discussion. While section 4 concludes the article.

## 2. PROPOSED METHOD

The suggested system is divided into the following steps: i) image preprocessing, ii) transfer learning, iii) feature extraction and finally, and iv) image retrieval. Figure 1 shows the process involved in the proposed methodology. The system consists of two phases, the training phase and the testing phase. The dataset used for this experiment is chest X-ray images with four classes namely COVID-19, normal, pneumonia-bacterial, and pneumonia-viral.

### 2.1. Image preprocessing

In the preprocessing phase of this study, the collection of a large chest X-ray dataset for COVID-19 diagnosis is done which includes two-step image augmentation and image enhancement. To guarantee uniformity across the collection, the training, and testing set images are downsized to  $224 \times 224$ , a typical dimension. Augmentation methods involve rotation range, height shift, width shift, shear range, zoom range, ZCA-whitening, feature-wise standard normalization, horizontal flip, and fill mode to overcome the class imbalance. These methods assisted in producing more samples and producing a dataset that was more evenly distributed. After augmenting the dataset, it was divided into various class segments, with an 80:20 ratio allocated to each class for both training and testing purposes. This division ensured that there were inclusive samples from every class in both the training and testing datasets.

These pre-processing steps have successfully enhanced the dataset’s diversity, balanced the class distribution, and created robust training and testing datasets. This study entailed the development and evaluation of deep learning models specifically designed for COVID-19 diagnosis, with these datasets serving as the fundamental basis. Image preprocessing also involves a technique to enhance the contrast of an image using LHE, as shown in Figure 2. Neighborhood adaptive local histogram equalization, or LHE, is used. Figure 2(a) is the original image, and Figure 2(b) is after-image enhancement using LHE. The contrast enhancement method known as LHE splits a picture into smaller, non-overlapping blocks or areas. Then it carries out separate histogram equalization inside each of these local neighborhoods.

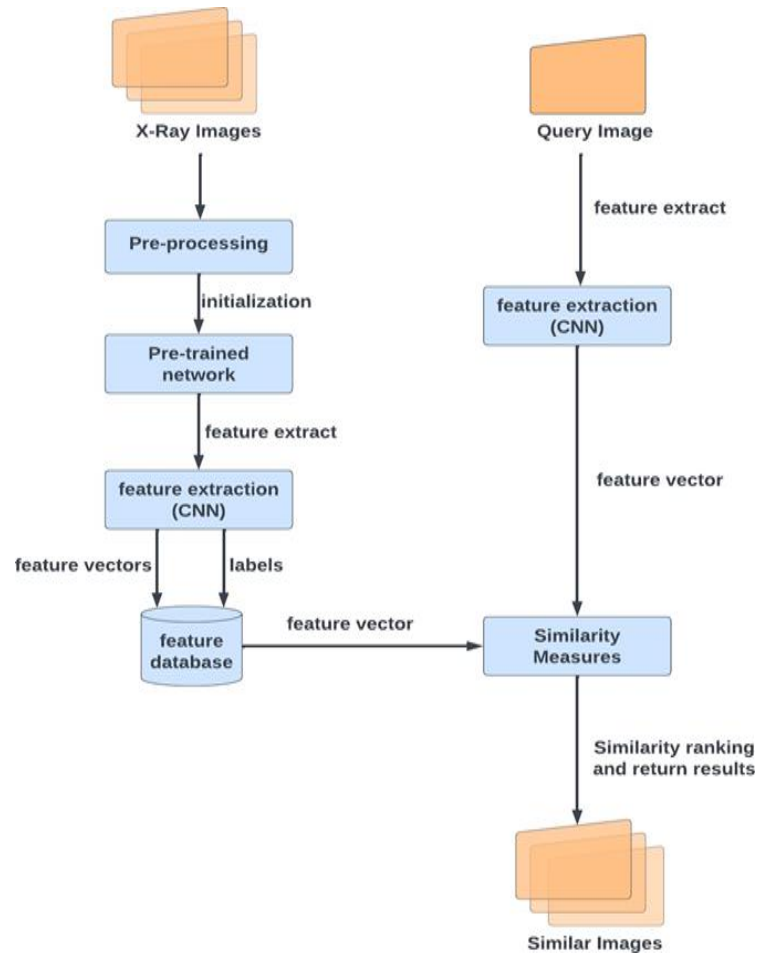


Figure 1. Proposed system for retrieving similar images

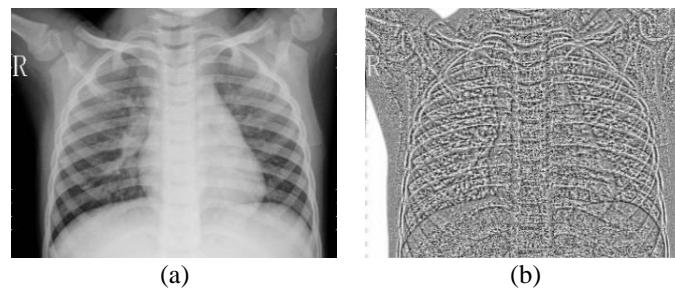


Figure 2. Applying local histogram equalization for contrast enhancement (a) original COVID image and (b) enhanced COVID image

## 2.2. Transfer learning

The study employs transfer learning as a powerful technique for the diagnosis of COVID-19. The model is specifically loaded with weights that were previously trained from the ImageNet dataset, which is a massive image categorization dataset. In computer vision tasks, initializing a deep neural network using ImageNet pre-trained weights and fine-tuning it for feature extraction is a popular and efficient method. Through this procedure, the extracted features from images are used in other applications by utilizing the extensive feature representations that have been learned from ImageNet. The learned parameters (weights and biases) of a neural network model that has been pre-trained on the ImageNet dataset are referred to as “ImageNet weights”. The information and feature representations that the model has learned throughout its training on ImageNet are represented by these weights.

### 2.3. Image feature extraction

This methodology employed an unsupervised technique for generating image feature vectors in a retrieval system. A deep neural network, like a CNN, is trained using the ImageNet dataset in the first training phase. The internal parameters of the model, such as its weights and biases, are changed during training through a technique known as gradient descent and backpropagation. The model's acquired weights may be used in other computer vision applications [27] once it has been trained on ImageNet. The proposed methodology incorporates an integral component called the "extract" function, which plays a pivotal role in capturing deep features from input images using the VGG-16 and DenseNet121 models. Typically, images in color are loaded into VGG-16 with 224×224 pixels as the fixed input size. There are a total of 13 convolutional layers in VGG-16. 3×3 kernels are used in all convolutional layers. As you move farther into the network, the number of filters steadily rises from a tiny starting point, creating an expanding receptive field. A max-pooling layer comes after two successive convolutional layers. By using a 2×2 window and a stride of 2, max-pooling reduces the dimension of the space by a factor of 2. Lastly, rectified linear unit (ReLU) for non-linearity, a flattened layer, and a fully connected layer1 that generates the feature vector of the input images. The DenseNet121 model contains an input size of 224×224. The convolutional layer consists of a kernel size of 5×5 and a stride of 2, with 4 dense blocks, and a 3×3 window max-pooling layer. DenseNet-121 is comprised of four dense blocks. A batch normalization layer, a ReLU activation function, and a 3×3 convolutional layer are all included in each dense unit. The transition layers consist of a batch normalization layer, a 1×1 convolution layer for the reduction of dimensionality, and a 2×2 average pooling layer. A global average pooling layer has been implemented at the network's end. The spatial dimensions are reduced to 1×1, resulting in a fixed-size mapping of features for every channel. Resulting in 4,096 features from the feature vector.

#### Algorithm 1. Image feature extraction and retrieval

Input: Training set, Query image

Output: Top-K closest images

Step 1: Load a pre-trained CNN model with ImageNet weights.

Step 2: Initialize an empty feature database.

Step 3: For each image 'I' in the training set: a) Resize 'I' to 224×224 pixels, b) Preprocess 'I' (LHE, transformations, normalization), c) Extract features from the chosen layer of the CNN model, and d) Store the extracted features in the feature database along with the image identifier.

Step 4: For each image 'I' in the test set: a) Resize the query image to 224×224 pixels, b) Preprocess the query image (LHE, transformations, normalization), and c) Extract features from the same layer used for training images.

Step 5: Initialize an empty similarity scores list.

Step 6: For each image 'I' in the feature database: a) compute the similarity score between the query image's features and 'I's features using a chosen distance metric (e.g., Euclidean distance, Manhattan similarity); b) Store the similarity score and the corresponding image identifier in the similarity scores list.

Step 7: Sort the similarity scores list in ascending order based on the computed similarity scores.

Step 8: Select the top-K images with the highest similarity scores from the feature database.

### 2.4. Image retrieval

To evaluate the similarity between images and gauge their likeness, the proposed method calculates the distances between their feature vectors using widely recognized similarity metrics such as Euclidean distance and Manhattan distance. Overall, this approach leveraged feature extraction, distance calculation using popular similarity measures shown in (1) and (2), and a structured distance matrix to facilitate image retrieval. Using this method, the system was able to find visually related images and show how well this strategy supports image-based queries and retrieval activities. Where  $i = 1, 2, \dots, n$  refers to the number of images and  $x, y$  are the coordinate values.

$$\text{Euclidean\_Distance}(x, y) = \sqrt{\sum_{i=1}^n (x_i - y_i)^2} \quad (1)$$

$$\text{Manhattan\_Distance}(x, y) = \|\mathbf{x} - \mathbf{y}\|_1 = \sum_{i=1}^n |x_i - y_i| \quad (2)$$

## 3. RESULTS AND DISCUSSION

### 3.1. Experimental setup

A GPU, cloud services, Windows OS (10 and above), Keras, TensorFlow, and Kaggle datasets are among the software tools and platforms that are exploited for this experiment. Specifically, the GPU used for this experiment is the Nvidia P100, which is available on the Kaggle Kernel platform. The project's hardware specifications can be met by a typical computer system, like the Dell Vostro 15 3000 with an Intel Core i5 processor.

### 3.2. Dataset description

The data set used for the suggested work was chest X-ray images separated into four types and collected from freely accessible medical databases. A total of 16,000 photos, 4,000 from each class, made up the dataset. According to Figure 3, the images were randomly divided into a training dataset and a testing dataset, with 80% and 20% of the total images going to each group. There were no overlapping images between the training set and testing set, which had different numbers of images at 12,800 and 3,200, respectively. Each class's photos were downsized to 224×224. Table 1 displays the breakdown of images used in the training dataset and testing dataset.

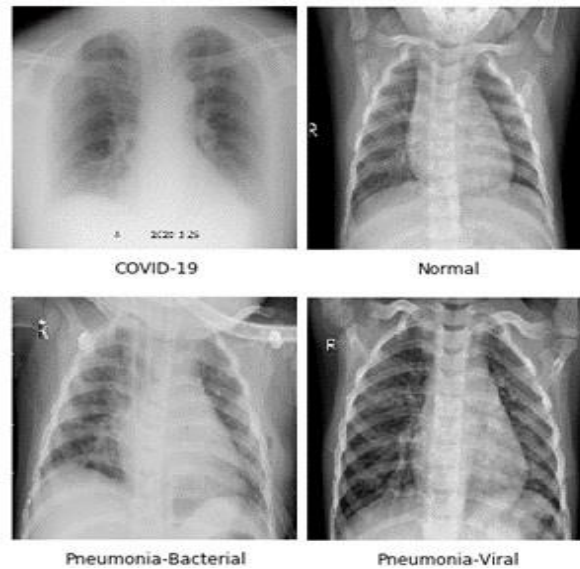


Figure 3. Sample images from the Chest X-ray dataset

Table 1. The chest X-Ray dataset description

Chest X-Ray Images	COVID-19	Normal	Pneumonia-Bacterial	Pneumonia-Viral
Training Set	3,200	3,200	3,200	3,200
Testing Set	800	800	800	800
Total	4,000	4,000	4,000	4,000

### 3.3. Performance measure

Assessing an image retrieval system involves evaluating retrieval results using various metrics and methodologies tailored to the task and system objectives. Typical assessment criteria include precision, which measures the ratio of relevant photos to all images retrieved, highlighting system correctness. Equations (3) and (4) introduce precision and recall, respectively. Precision gauges the percentage of relevant photos among retrieved results, while recall assesses retrieval comprehensiveness by comparing successfully retrieved relevant photos to the total relevant images in the dataset.

$$\text{Precision} = \frac{\text{Number of relevant images retrieved}}{\text{Number of retrieved images}} \quad (3)$$

$$\text{Recall} = \frac{\text{No of relevant images retrieved}}{\text{Total No of relevant images in database}} \quad (4)$$

#### 3.3.1. Top-k retrieval

This metric evaluates the accuracy of the retrieval system at a specific threshold point (k), where k represents the number of top-ranked images successfully recovered. By checking if relevant images are within the top-k retrieved results for each query, we estimate top-k accuracy. Tables 2 and 3 present the results of top-k retrieval using Euclidean and Manhattan distances for the DenseNet121 and VGG-16 models, respectively. Generally, the top-k results using the Manhattan distance measure on the DenseNet121 model outperform those of the VGG-16 model.

Table 2. Top-k retrieval using Euclidean and Manhattan distance measures for the DenseNet121 model

Query Images	Distance Metric	Top-10%	Top-20%	Top-30%	Top-40%
COVID-19	Euclidean	96.2	95.5	95.2	94.8
Normal		96.6	95.9	95.6	95.2
Pneumonia-bacterial	Manhattan	82.4	82.1	81.7	81.4
Pneumonia-viral		80.9	79.8	78.9	78.3
COVID-19		97.1	96.4	96.1	95.9
Normal		96.8	96.5	96.2	95.9
Pneumonia-bacterial		82.4	82.1	81.7	81.4
Pneumonia-viral		81.7	80.1	79.1	78.6

Table 3. Top-k retrieval using Euclidean and Manhattan distance measures for the VGG-16 model

Query Images	Distance Metric	Top-10%	Top-20%	Top-30%	Top-40%
COVID-19	Euclidean	97	96.4	96.1	95.9
Normal		93.3	92.1	91.4	90.6
Pneumonia-bacterial	Manhattan	77.7	76.3	75.7	75.3
Pneumonia-viral		80.2	78.9	78.4	77.9
COVID-19		97.8	97.1	96.7	96.4
Normal		93.1	92.8	92.1	95.9
Pneumonia-bacterial		77.8	77.5	75.8	75.3
Pneumonia-viral		80.9	79.1	78.7	78.1

3.3.2. Precision and recall

Precision and recall represent crucial evaluation measures employed in information retrieval. They serve to assess model performance, especially in scenarios involving binary classification tasks. These metrics find particular utility when addressing imbalanced datasets or situations where the significance of one class outweighs the other. Using the precision and recall measurement metrics, we compute the retrieval system’s performance using VGG-16 and DenseNet121. Retrieval performance about precision and recall for the DenseNet121 model and VGG-16 using Manhattan distance measure on four different classes, namely COVID, normal, bacterial, and viral, is presented in Figure 4 (a) and 4(b), respectively. Overall, the average precision vs. recall results in Figure 4(a) are 82.26% for COVID-19, 81.66% for normal, 67.32% for pneumonia-bacterial, and 61.03% for pneumonia-viral. Whereas the average precision vs. recall in Figure 4(b) is 81.83% for COVID-19, 68.02% for normal, 64.3% for pneumonia, and 60.37% for pneumonia-viral.

For a given query image from the COVID-19 class, the top 10 retrieved images using DenseNet121 and Manhattan distance are shown in Figure 5. In Figure 5(a), we have a query image belonging to the COVID-19 class and the top 10 images retrieved based on the distances sorted in ascending order along with the image ID using DenseNet121. Similarly, Figure 5(b), 5(c), and 5(d) are the results for the normal, pneumonia-bacterial, and pneumonia-viral classes, respectively. The total number of similar images retried from Figure 5(a) is 10, Figure 5(b) is 10, Figure 5(c) is 10, and Figure 5(d) is 9. Due to their parallel processing capabilities, speed, support for deep learning, and capacity to handle large datasets, GPUs are well-suited for feature extraction in CBMIR tasks. They are crucial in increasing the efficiency and responsiveness of CBIR systems, particularly in real-time or high-throughput applications. Table 4. compares the feature extraction time using GPUs on VGG-16 and DenseNet121. DenseNet121 on GPUs consumes less time for extracting the features of large medical image datasets.

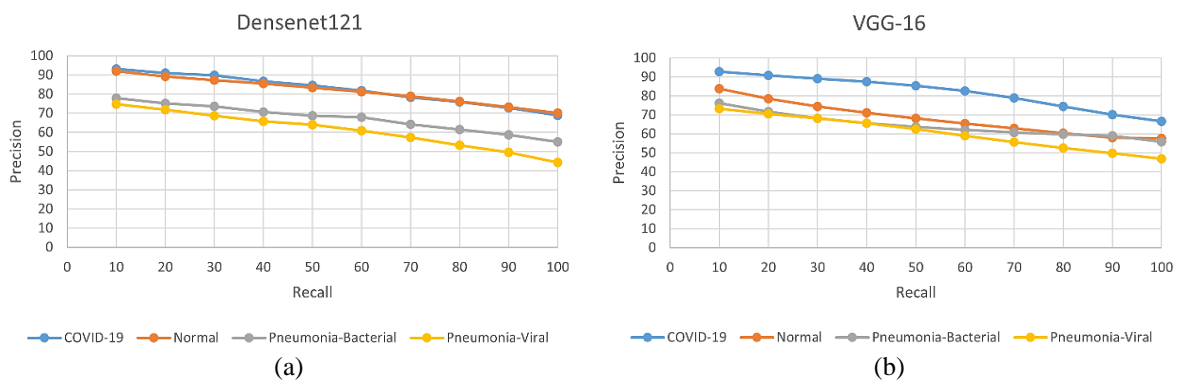


Figure 4. Precision vs recall results for (a) DenseNet121 and (b) VGG-16



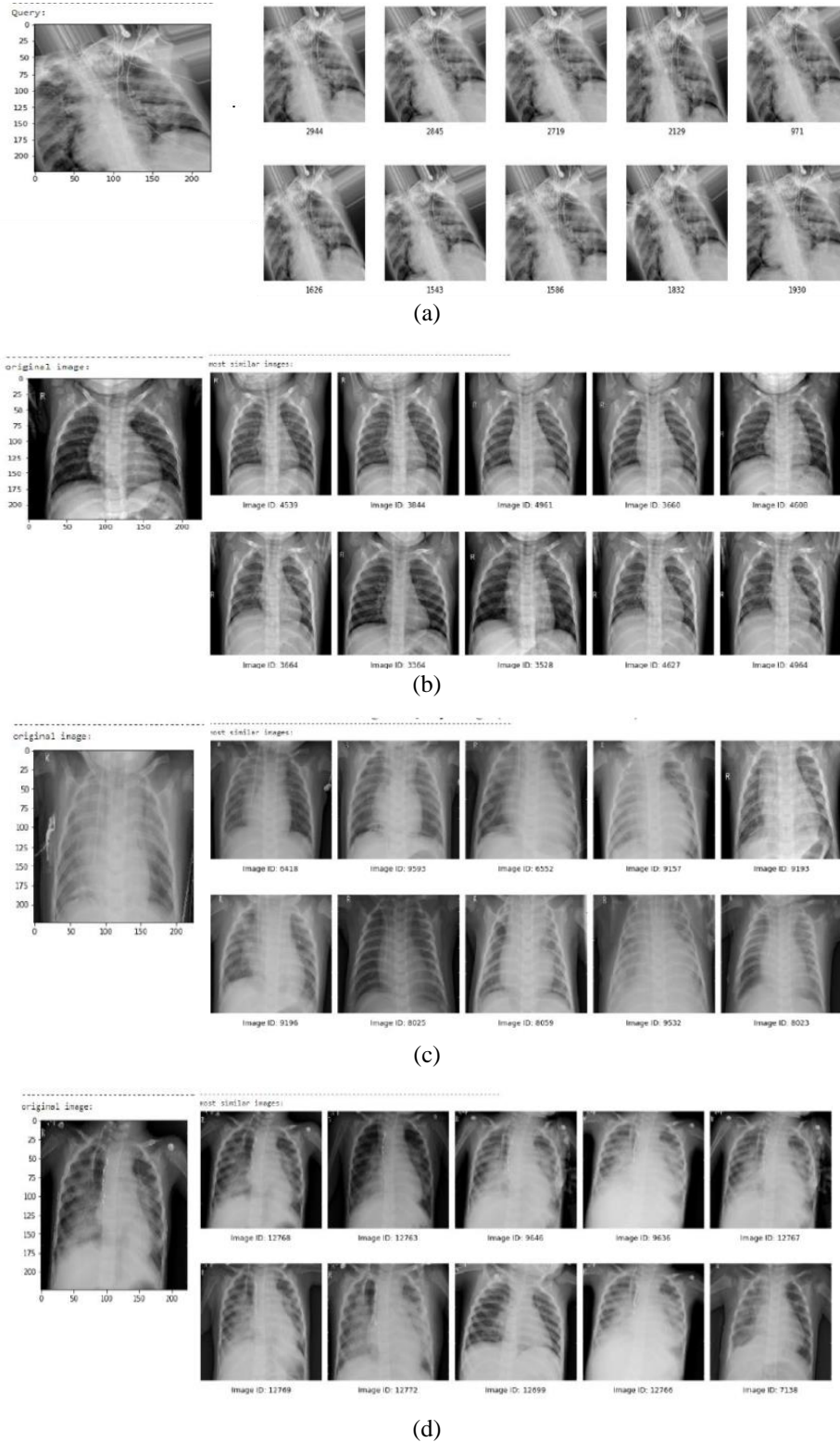


Figure 5. Results of the sample query image and top-10 similar images belonging to (a) COVID-19, (b) normal, (c) pneumonia-bacterial, (d) pneumonia-viral

Table 4. Comparison of feature extraction time using GPUs on CNN models

Proposed CNN Model	Time Taken for feature extraction on GPUs
VGG-16	42m 17s
DenseNet121	13m 21s

#### 4. CONCLUSION

The suggested approach provides a unique method for discriminating COVID-19 patients from viral pneumonia using chest X-ray images. The proposed method leverages the power of LHE for image enhancement and VGG16 and DenseNet121 deep learning models to retrieve relevant and comparable examples from a vast dataset of chest X-ray images. The experiment uses various similarity metrics, including Euclidean and Manhattan distances, and observed that the Manhattan distance yielded superior results for the top 10 retrievals. Furthermore, a comparison between the VGG16 and DenseNet121 models found that, when using the Manhattan distance metric, the DenseNet121 model on GPUs outperformed, achieving top-10 retrieval rates of 97.13% for COVID-19, 96.84% for normal, 82.63% for pneumonia-bacterial, and 81.72% for pneumonia-viral, and precision@recall10 of 93.14% for COVID-19, 91.88% for normal, 77.84% for Pneumonia-bacterial, and 74.71% for Pneumonia-viral. The suggested method has the potential to assist radiologists with everyday tasks, especially in the context of the present COVID-19 pandemic. In the future, the suggested system aims to expand its capabilities by incorporating the ability to assess the severity of COVID-19 and pneumonia cases. We aim to enhance the model's precision and speed by harnessing computational resources like parallel GPUs.

#### REFERENCES




- [1] N. Chen *et al.*, "Epidemiological and clinical characteristics of 99 cases of 2019 novel coronavirus pneumonia in Wuhan, China: a descriptive study," *The Lancet*, vol. 395, no. 10223, pp. 507–513, Feb. 2020, doi: 10.1016/S0140-6736(20)30211-7.
- [2] A. Shoebati *et al.*, "Automated detection and forecasting of COVID-19 using deep learning techniques: A review," *Neurocomputing*, vol. 577, Apr. 2024, doi: 10.1016/j.neucom.2024.127317.
- [3] M. Q. Shatnawi, M. Alrousan, and S. Amareen, "A new approach for content-based image retrieval for medical applications using low-level image descriptors," *International Journal of Electrical and Computer Engineering (IJECE)*, vol. 10, no. 4, pp. 4363–4371, Aug. 2020, doi: 10.11591/ijece.v10i4.pp4363-4371.
- [4] N. Arora, A. Kakde, and S. C. Sharma, "An optimal approach for content-based image retrieval using deep learning on COVID-19 and pneumonia X-ray Images," *International Journal of System Assurance Engineering and Management*, vol. 14, no. 1, pp. 246–255, Dec. 2023, doi: 10.1007/s13198-022-01846-4.
- [5] R. Shetty, V. S. Bhat, and J. Pujari, "Survey on techniques and image modalities in content based medical image retrieval," *International Journal of Scientific Research in Computer Science, Engineering and Information Technology*, pp. 10–20, Mar. 2022, doi: 10.32628/cseit228147.
- [6] S. Agrawal, A. Chowdhary, S. Agarwala, V. Mayya, and S. Kamath, "Content-based medical image retrieval system for lung diseases using deep CNNs," *International Journal of Information Technology (Singapore)*, vol. 14, no. 7, pp. 3619–3627, Jun. 2022, doi: 10.1007/s41870-022-01007-7.
- [7] C. Muramatsu, "Overview on subjective similarity of images for content-based medical image retrieval," *Radiological Physics and Technology*, vol. 11, no. 2, pp. 109–124, May 2018, doi: 10.1007/s12194-018-0461-6.
- [8] N. K. Ibrahim, A. H. Al-Saleh, and A. S. A. Jabar, "Texture and pixel intensity characterization-based image segmentation with morphology and watershed techniques," *Indonesian Journal of Electrical Engineering and Computer Science (IJECS)*, vol. 31, no. 3, pp. 1464–1477, Sep. 2023, doi: 10.11591/ijeecs.v31.i3.pp1464-1477.
- [9] A. Zhong *et al.*, "Deep metric learning-based image retrieval system for chest radiograph and its clinical applications in COVID-19," *Medical Image Analysis*, vol. 70, May 2021, doi: 10.1016/j.media.2021.101993.
- [10] S. Mohagheghi, M. Alizadeh, S. M. Safavi, A. H. Foruzan, and Y. W. Chen, "Integration of CNN, CBMR, and visualization techniques for diagnosis and quantification of COVID-19 disease," *IEEE Journal of Biomedical and Health Informatics*, vol. 25, no. 6, pp. 1873–1880, Jun. 2021, doi: 10.1109/JBHI.2021.3067333.
- [11] A. Belalia, K. Belloulata, and S. Zhu, "Efficient histogram for region based image retrieval in thdiscrete cosine transform domain," *IAES International Journal of Artificial Intelligence (IJ-AI)*, vol. 11, no. 2, pp. 546–563, Jun. 2022, doi: 10.11591/ijai.v11.i2.pp546-563.
- [12] O. A. Adegbola, I. A. Adeyemo, F. A. Semire, S. I. Popoola, and A. A. Atayero, "A principal component analysis-based feature dimensionality reduction scheme for content-based image retrieval system," *Telkomnika (Telecommunication Computing Electronics and Control)*, vol. 18, no. 4, pp. 1892–1896, Aug. 2020, doi: 10.12928/TELKOMNIKA.V18I4.11176.
- [13] M. A. Salam, S. Taha, and M. Ramadan, "COVID-19 detection using federated machine learning," *PLoS ONE*, vol. 16, Jun. 2021, doi: 10.1371/journal.pone.0252573.
- [14] A. A. Abdulmunem, Z. A. Abutiheen, and H. J. Aleqabie, "Recognition of Corona virus disease (COVID-19) using deep learning network," *International Journal of Electrical and Computer Engineering (IJECE)*, vol. 11, no. 1, pp. 365–374, Feb. 2021, doi: 10.11591/ijece.v11i1.pp365-374.
- [15] B. Hu, B. Vasu, and A. Hoogs, "X-MIR: EXplainable medical image retrieval," in *2022 IEEE/CVF Winter Conference on Applications of Computer Vision (WACV)*, Jan. 2022, pp. 1544–1554, doi: 10.1109/WACV51458.2022.00161.
- [16] R. Shetty, V. S. Bhat, S. Handigol, S. Kumar, S. Kubasad, and K. Badiger, "Medical image retrieval system for endoscopy images using CNN," Jun. 2023, doi: 10.1109/ICAISC58445.2023.10199908.
- [17] T. Asmaria, D. A. Mayasari, A. D. G. Febrananda, N. Nurul, A. J. Rahyussalim, and I. Kartika, "Computed tomography image analysis for Indonesian total hip arthroplasty designs," *International Journal of Electrical and Computer Engineering (IJECE)*, vol. 12, no. 6, pp. 6123–6131, Dec. 2022, doi: 10.11591/ijece.v12i6.pp6123-6131.
- [18] M. K. Alsmadi *et al.*, "Susceptible exposed infectious recovered-machine learning for COVID-19 prediction in Saudi Arabia," *International Journal of Electrical and Computer Engineering (IJECE)*, vol. 13, no. 4, pp. 4761–4776, Aug. 2023, doi: 10.11591/ijece.v13i4.pp4761-4776.
- [19] G. Wu, W. Lu, G. Gao, C. Zhao, and J. Liu, "Regional deep learning model for visual tracking," *Neurocomputing*, vol. 175, pp. 310–323, Jan. 2015, doi: 10.1016/j.neucom.2015.10.064.
- [20] G. Hinton *et al.*, "Deep neural networks for acoustic modeling in speech recognition: the shared views of four research groups," *IEEE Signal Processing Magazine*, vol. 29, no. 6, pp. 82–97, Nov. 2012, doi: 10.1109/MSP.2012.2205597.
- [21] I. Lauriola, A. Lavelli, and F. Aiolfi, "An introduction to deep learning in natural language processing: models, techniques, and






- tools,” *Neurocomputing*, vol. 470, pp. 443–456, Jan. 2022, doi: 10.1016/j.neucom.2021.05.103.
- [22] Z. Yan *et al.*, “Multi-instance deep learning: discover discriminative local anatomies for bodypart recognition,” *IEEE Transactions on Medical Imaging*, vol. 35, no. 5, pp. 1332–1343, May 2016, doi: 10.1109/TMI.2016.2524985.
- [23] P. N. Murthy and S. K. Y. Hanumanthaiah, “A simplified and novel technique to retrieve color images from hand-drawn sketch by human,” *International Journal of Electrical and Computer Engineering (IJECE)*, vol. 12, no. 6, pp. 6140–6148, Dec. 2022, doi: 10.11591/ijece.v12i6.pp6140-6148.
- [24] M. K. N. Mursalin and A. Kurniawan, “Multi-kernel CNN block-based detection for COVID-19 with imbalance dataset,” *International Journal of Electrical and Computer Engineering (IJECE)*, vol. 11, no. 3, pp. 2467–2476, Jun. 2021, doi: 10.11591/ijece.v11i3.pp2467-2476.
- [25] M. Loey, S. El-Sappagh, and S. Mirjalili, “Bayesian-based optimized deep learning model to detect COVID-19 patients using chest X-ray image data,” *Computers in Biology and Medicine*, vol. 142, Mar. 2022, doi: 10.1016/j.compbiomed.2022.105213.
- [26] M. A. Elaziz, K. M. Hosny, A. Salah, M. M. Darwish, S. Lu, and A. T. Sahlol, “New machine learning method for imagebased diagnosis of COVID-19,” *PLoS ONE*, vol. 15, no. 6, Jun. 2020, doi: 10.1371/journal.pone.0235187.
- [27] S. Yakin, T. Hasanuddin, and N. Kurniati, “Application of content based image retrieval in digital image search system,” *Bulletin of Electrical Engineering and Informatics (BEEI)*, vol. 10, no. 2, pp. 1122–1128, Apr. 2021, doi: 10.11591/EEI.V10I2.2713.

## BIOGRAPHIES OF AUTHORS






**Rani Shetty**    is an assistant professor at SDM College of Engineering and Technology, Department of Computer Science, Dharwad, India. She received a B.E. in computer science from REC, Hulkoti, M.Tech. in computer science from SDM College, Dharwad. She is currently pursuing her Ph.D. in computer engineering with a specialization in medical image retrieval at Visvesvaraya Technological University, Karnataka, India. Her research areas are image processing, pattern recognition, and medical image analysis. She has been an active member of IEEE since 2019. She can be contacted at email: ranishetty1990@sdmct.ac.in.






**Vandana S. Bhat**    is an assistant professor at SDM College of Engineering and Technology, Department of Artificial Intelligence and Machine Learning, SDM College of Engineering and Technology, Dharwad, India. She received her M.Tech in computer cognition and technology from the University of Mysore and Ph.D. in computer science and engineering from VTU Belagavi. She has supervised more than 10 PG students and 4 Ph.D. students of which 2 have completed. She has authored a book titled “Microarray Image Denoising” Lambert Academic Publishers. She has authored or co-authored more than 30 publications: 10 proceedings, 18 international journals, and 2 national journals. Her research interests include artificial intelligence and machine learning, image processing, and database management systems. She can be contacted at vandana.bhat@sdmct.ac.in.



**Jagadeesh Pujari**    is a professor and head of the Department of Information Science and Engineering, SDM College of Engineering and Technology, Dharwad, India. He received his B.E. in computer science from SDM College, Dharwad and Ph.D. from the University of Gulbarga, Karnataka, India. He has an experience of 32 years in research, academics, and industry. His research interests span image processing, pattern recognition, big data analytics, and machine learning. He has wide publications in reputed international conferences and journals. He has supervised 8 Ph.D. and more than 80 postgraduate students. He is the investigator for several projects funded by the Government of India and Industries. He can be contacted at jdpujari@sdmct.ac.in.



**Rashmi Shetty**    is a senior resident at Kasturba Medical College, Department of Pathology, Manipal. She received an MD in pathology from VIMS, Bellari, a DNB from NBE, New Delhi, and an MBBS from KIMS, Hubli, India. Her area of interest is teaching programs involving undergraduates - MBBS, BDS, and Allied health science students and postgraduates. Areas of expertise are diagnostics—clinical pathology, hematology, cytopathology, histopathology, and immunohistochemistry. She can be contacted at email: shetty.rashmi@manipal.edu.